

Selection of High-Performance Working Fluid for a Solar-Geothermal Absorption Cooling System and Techno-Economic Study in the Northern Mexican Conditions

Amín Altamirano*, Benoît Stutz, Nolwenn Le Pierrès

LOCIE Laboratory, Université Savoie Mont Blanc, CNRS UMR5271, Savoie Technolac, 73376 Le Bourget Du Lac (France)

Abstract

The global energy demand is increasing at alarming rates. This increase is expected to be twice as big in developed countries like Mexico, and until 2040, most of this energy will still be coming from fossil fuels, which generate pollution and global warming, increasing even more the energy demand and creating a vicious circle. Absorption systems represent a possibility to contribute to the reduction of fossil fuels consumption and CO₂ emissions. These systems can run on renewable energies like solar energy, however, they possess until now high initial investment costs. Two studied methods to improve these system's effectiveness are new refrigerants and heat sink sources. The present article proposes the study of a small-capacity geothermally cooled absorption system in the Monterrey city (Mexico) climate conditions comparing the two more conventional working fluids (NH₃-H₂O and H₂O-LiBr) and an innovative working fluid (NH₃-LiNO₃). The work is divided into three parts: The first section studies the specific climatic conditions of Monterrey and their impact on the operating temperatures in the system. The second section compares the thermodynamic cycles of the three proposed working fluids in these conditions. Finally, the dimensioning of the components of the system and an economic viability study for the three working pairs is presented to see if it is cost-effective.

Keywords: Absorption system, ammonia, water, lithium bromide, lithium nitrate, HGHE

1. Introduction

The global energy demand is increasing at alarming rates. According to the International Energy Agency, the increase in the global energy demand between 2000 and 2040 is expected to be of around 70%, and from the total energy consumed in 2040, 74% will still be coming from fossil fuels, whose combustion generates pollution and global warming (IEA, 2016). Moreover, due to human activity, there is an expected increase in the global average temperature in the range of 1.4 to 5.8°C for 2100 compared to 1990 (Aliane et al., 2016), which will impact even more the biggest contributor to world energy consumption and greenhouse emissions: the building sector (Allouhi et al., 2015). This increase in the cooling demand due to global warming generates even more energy consumption, generating a vicious circle that can only be stopped with the transition to clean energies. Nowadays, in the US, 40% of electricity during the summer is consumed by commercial buildings for air conditioning (AC) purposes (Agrouaz et al., 2017). New international agreements require the development of systems that contribute to the fight against climate change and global warming (Calm, 2008).

Absorption systems replace the mechanical compression of standard refrigeration systems by chemical compression. These systems are still more expensive than common vapor compression systems. However, they will be of great interest in the coming years because they are able to run from renewable heat and waste heat (Dube et al., 2017), which could importantly contribute to the reduction of fossil fuel consumption and harmful emissions to the environment (Wu et al., 2014a). When solar driven, the need for cooling coincides with the time of higher irradiation levels. Moreover, absorption systems are gaining acceptance and seem like a real alternative for cooling residential, light commercial and industrial applications (Zhu and Gu, 2010). Their low operating cost has made them more attractive in recent years (Wu et al., 2014a). The main advantage of absorption cooling systems over the other heat driven cooling technologies is their higher COP (Hassan and Mohamad, 2012).

Nomenclature		<i>Greek letters</i>	
A	solar thermal collector area (m ²)	η_0	solar thermal collector optical efficiency
<i>a</i>	thermal diffusivity (m ² s ⁻¹)	η_{col}	solar thermal collector efficiency
<i>a</i> ₁	linear coefficient of the solar thermal collector	θ	inclination angle of the solar thermal panel (°)
<i>a</i> ₂	quadratic coefficient of the solar thermal collector	ω	annual pulse (rad/s)
COP	coefficient of performance		
CR	circulation ratio		
<i>G</i> [*]	solar irradiation (Wm ⁻²)		
<i>h</i>	specific enthalpy (kJ kg ⁻¹)		
<i>k</i> (θ)	solar thermal collector tilt angle factor		
<i>m</i>	mass flow rate (kg s ⁻¹)		
\dot{Q}	exchanged heat (kW)		
<i>T</i>	temperature (K)		
<i>T</i> _{amp}	yearly amplitude of the ground-level temperature (K)		
<i>T</i> _a	ambient temperature (K)		
<i>T</i> _{mean}	mean ground temperature (K)		
<i>T</i> _m	average temperature of the fluid in the solar collector (K)		
<i>t</i>	observed day of the year (s)		
<i>t</i> _c	coldest day (s)		
\dot{W}	mechanical work transfer to or from the component (kW)		
<i>x</i>	absorbent solution mass fraction		
<i>z</i>	depth (m)		
		<i>Subscripts</i>	
		<i>a</i>	absorber
		<i>c</i>	condenser
		<i>col</i>	collector
		<i>e</i>	evaporator
		<i>i</i>	in
		<i>int</i>	intermediate
		<i>g</i>	generator
		<i>p</i>	pump
		<i>o</i>	out
		<i>Accentuation</i>	
		~	undisturbed by the exchanger

Considering their thermodynamic cycle arrangement, absorption refrigeration systems can be divided into three categories: single effect, half-effect and double effect (or multi-effect) cycles. The single-effect cycle requires lower temperatures compared to the multi-effect cycles (Aliane et al., 2016) and is the most advantageous in terms of cost and simple configuration (Hassan and Mohamad, 2012). At the same time, it is the most commercially available. Two absorption pairs are commonly encountered: H₂O-LiBr (Water-Lithium Bromide) and NH₃-H₂O (Ammonia-Water).

Nowadays, different research teams focus on improving absorption systems to reduce the manufacturing costs, complexity, maintenance, and environmental concerns. One challenge is the search for the ideal refrigerant, for which, besides of good thermal properties, special attention to its environmental impact has gained attention in recent years (Calm, 2008). Other research groups are investigating alternative heat sink possibilities, as cooling towers present some disadvantages like high water consumption, high maintenance needs, electricity consumption, and there have been reported cases of legionella bacteria development (Bailo et al., 2010; Monné et al., 2011). Air-cooled systems have been investigated and experimented. However, these systems require higher driving temperatures and get closer to the crystallization line in the case of the H₂O-LiBr working pair. Moreover, their performance is influenced by the highly variable ambient temperature (Chen et al., 2017). Geothermal heat exchangers (GHE) have recently been proposed as heat sinks for absorption systems. They possess some advantages compared to the conventional ones in terms of efficiency, operating costs, and maintenance (Noorollahi et al., 2018). Borehole heat exchangers are the most common GHE, while other options like pile GHE or horizontal loop GHE also exist, all of which present disadvantages in terms of cost or surface required (Moch et al., 2014). Helical geothermal heat exchangers (HGHE) have recently been proposed as they offer a good compromise between borehole heat exchangers and horizontal loops in terms of required surface and cost. However, there are very few studies that investigate their operation (Moch et al., 2015).

The present work proposes the study of a small-capacity geothermally cooled absorption system for hot climates (Figure 1). To be more precise, the climatic and economic conditions taken into account for the present study are the ones from the Monterrey city, in northern Mexico, as it is a representative city of this region in which the need for AC and the irradiation levels are both very high. The study is divided into three parts. In the first part, the study of the specific climatic conditions and determination of the underground temperature profile of the Monterrey zone is done. This information is used to determine the operating equilibrium intermediate and generator temperatures in the absorption system and a comparison of the thermodynamic cycle performances of three working fluids is performed in a second section. Two of the compared working fluids are the conventional NH₃-H₂O and H₂O-LiBr pairs, while

the third working fluid is the recently studied NH₃-LiNO₃ working pair. Finally, in the third part, the dimensioning of the components of the system is done for the three selected working fluids. An economic assessment is presented at the end to analyze the economic viability of the proposed systems.

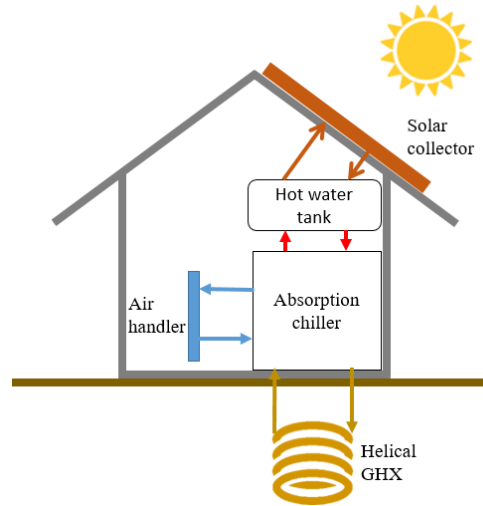


Fig. 1: Diagram of the proposed solar-geothermal absorption cooling system.

2. Climatic conditions and ground temperature profiles

Monterrey is the 3rd largest metropolitan area in Mexico. To determine the operating temperature profiles of the machine, data from the Mexican National Meteorological System (SMN, 2018) and the Integral System of Environmental Monitoring (SIMA, 2018) were used. This data is illustrated in Figure 2.

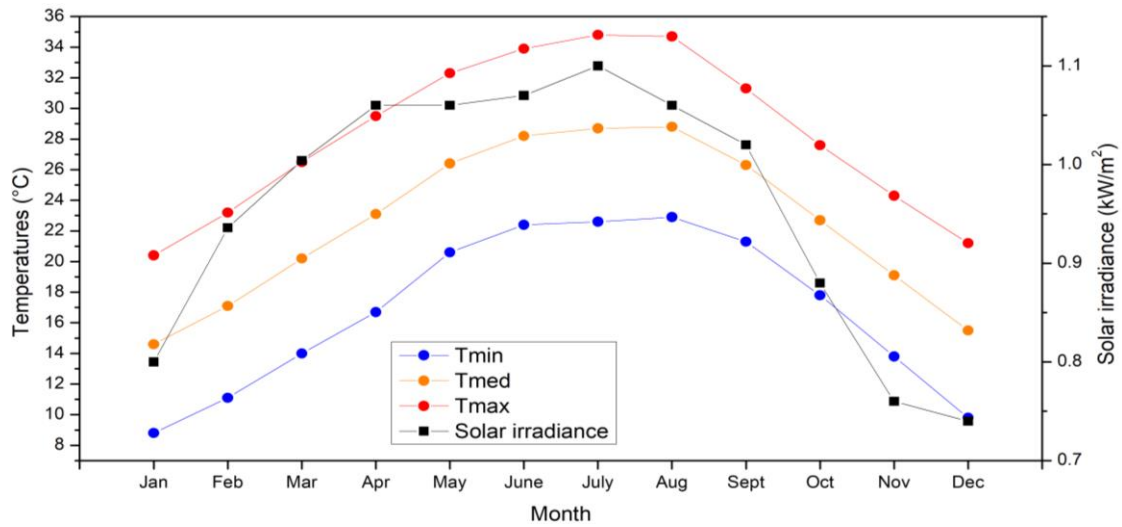


Fig. 2: Monterrey city maximum solar irradiance in 2017 (SIMA, 2018) and temperature profiles from 1981 to 2010 (SMN, 2018).

Considering the underground as a semi-infinite solid, spatially homogeneous, with thermal transfers only occurring by conduction, the underground undisturbed temperature profile can be obtained by equation 1 (Doughty et al., 1991). This equation allows to represent graphically the undisturbed underground temperature profiles in Monterrey for the different seasons, as observed in Figure 3.

$$\tilde{T}(z, t) = T_{mean} - T_{amp} \exp\left(z \sqrt{\frac{\omega}{2a}}\right) \cos\left(\omega(t - t_c) + z \sqrt{\frac{\omega}{2a}}\right) \quad (\text{eq. 1})$$

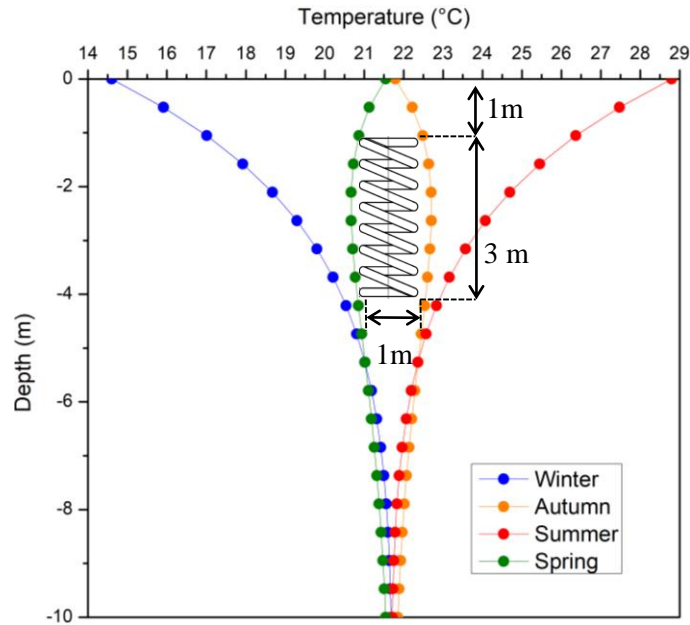


Fig. 3: Underground temperature profile of Monterrey city for different seasons.

Models available in the literature often don't take into account the effect of the distance between the HGHE coils and the local variations in temperature due to the heat transfer between the heat exchangers and the ground, which usually leads to unrealistic calculations (Agbossou et al., 2018). In the present study, these effects are taken into account to obtain more realistic results. HGHE usually have heights between 2 and 6 m, and diameters between 0.35 and 2 m. Their upper part generally being placed at 1 m below the ground level (Moch et al., 2014). In the present study, HGHE coils of 1 m diameter and 3 m height inserted in a 4 m deep were selected. Considering the hottest days during summer, the average undisturbed underground temperature is about 24°C (the temperature of the undisturbed ground being enclosed between 26.3°C at 1 m depth and 22.7°C at 4 m depth). The increase of the underground temperature due to the heat released by the absorption system is estimated to be of around 9°C during the hottest day using transient simulations (see Section 4.1). Considering a temperature difference of 2°C between the underground and the heat transfer fluid, and a difference of 5°C between the heat transfer fluid and the fluids in the absorption machine, an equilibrium outlet intermediate temperature for the absorption system of around 40°C is assumed (see Figure 4). While thanks to the irradiation levels during sunny days, equilibrium outlet generator temperatures in the range of 70-90°C (see Figure 4) can be achieved with flat solar collectors and a non-pressurized water tank for the hot source.

3. Thermodynamic comparison of the working fluids

2.1. Description of the system

The simulated geometry is illustrated in Figure 4. It consists of an evaporator, a condenser, an absorber, a generator, a solution pump, a solution heat exchanger (SHX) and two valves. In the case of the $\text{NH}_3\text{-H}_2\text{O}$ system, a rectifier is needed after the generator, however, in the case of the $\text{NH}_3\text{-LiNO}_3$ and $\text{H}_2\text{O-LiBr}$ working pairs, the rectifier is eliminated of the diagram and points 11 and 12 disappear. The solution in the generator is heated and desorbs refrigerant vapor. This vapor is condensed at the condenser before passing through an expansion valve and being vaporized again at a lower pressure and a lower temperature in the evaporator. The evaporation heat is taken from the cold source. The vapor produced at the evaporator is absorbed by the highly concentrated solution in the absorber. The resulting diluted solution is pumped from the absorber to the generator, where the cycle starts again (Best and Rivera, 2015). A Solution Heat Exchanger (SHX) is added between the absorber and the generator to increase the efficiency of the machine by recovering internal heat.

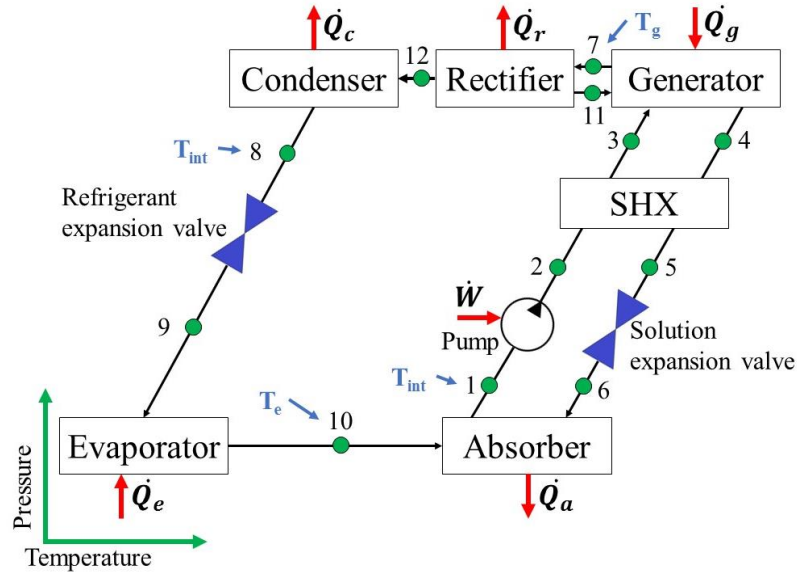


Fig. 4: Studied geometry of NH₃-H₂O single stage absorption cooling system (for the NH₃-LiNO₃ and H₂O-LiBr working fluids, the rectifier is eliminated and points 11 and 12 disappear).

For this study, the two most conventional working fluids in absorption systems (NH₃-H₂O and H₂O-LiBr) and one innovative working fluid (NH₃-LiNO₃) were selected. Water as refrigerant presents different advantages like a high enthalpy of vaporization, high availability, low-cost, and environmental friendliness. The H₂O-LiBr solution offers a high purity of refrigerant at the exit of the generator and high COP compared to the NH₃-H₂O system. However, there are some disadvantages of using water as refrigerant. For example, it is restricted to positive cooling and it operates in vacuum conditions, which requires special expensive components. Moreover, there are some corrosion and crystallization risks. NH₃ also possesses a high enthalpy of evaporation. Moreover, this refrigerant allows negative cooling and moderate working pressures, however, it is toxic. In the case of the NH₃-H₂O pair, the properties and materials compatibility are well documented and there are no crystallization risks. However, a supplementary component is required (a rectifier, Figure 4) to improve the refrigerant purity (Ullah et al., 2013). The system has a lower COP compared to the H₂O-LiBr working pair, and it is also an alkaline and corrosive solution. Finally, the NH₃-LiNO₃ is a recently studied working pair, which eliminates the disadvantages of the NH₃-H₂O solution, as it does not require a rectifier, it has a higher COP than the NH₃-H₂O working pair, and there are very low crystallization risks. Moreover, it is non-corrosive to steel. However, experimental results have shown a limited performance due to an elevated viscosity (Cera-Manjarres et al., 2018; Wu et al., 2014a).

2.2 Assumptions for the thermodynamic analysis

The assumptions that were taken into account to develop the simulations and analysis for the studied systems are as follows:

- The system operates under steady conditions.
- Pressure losses due to friction in the components and pipes are considered negligible.
- The refrigerant at the outlet of the condenser and evaporator (points 8 and 10 in Figure 4) is under saturated conditions.
- The solution at the outlet of the generator and the absorber (points 1 and 7 in Figure 4) is under equilibrium conditions.
- The heat losses to the surroundings are considered negligible.
- The cooling capacity remains constant at $\dot{Q}_e = 5$ kW.
- The evaporator outlet temperature remains constant at $T_{ev} = 10^\circ\text{C}$ (point 10 in Figure 4).
- The SHX effectiveness is fixed at 0.8.
- For the NH₃-H₂O working pair, an ideal rectifier (thermodynamically reversible) was considered, which in simple terms leads to $T_{11}=T_7$ and $x_{11}=x_3$.

2.3 Thermodynamic analysis

Thermophysical properties of the studied working pairs are needed to calculate the performance of the proposed absorption refrigeration cycle. The thermophysical properties of pure ammonia were obtained from Tillner-Roth et al. (1993). In the case of the $\text{NH}_3\text{-LiNO}_3$ solution, the last correlations for the equilibrium pressure and isobaric specific heat were presented by Hernández-Magallanes et al. (2017), and the specific enthalpy was obtained from Farshi et al. (2014). The $\text{H}_2\text{O-LiBr}$ properties were obtained from Pátek and Klomfar (2006). Finally, the thermodynamic properties of the $\text{NH}_3\text{-H}_2\text{O}$ solution were obtained from Ibrahim and Klein (1993).

A mathematical model was developed based on the mass and energy balances for each component in the absorption cycle. The main equations used in the model were the total mass conservation (equation 2), the absorbent conservation (equation 3), the energy balance for each of the components (equation 4), the coefficient of performance (equation 5), and the circulation rate (equation 6).

$$\sum m_i = \sum m_o \quad (\text{eq. 2})$$

$$\sum(m_i x_i) = \sum(m_o x_o) \quad (\text{eq. 3})$$

$$\sum((m_i h_i) - (m_o h_o)) + \sum(\dot{Q}_i - \dot{Q}_o) + \dot{W} = 0 \quad (\text{eq. 4})$$

$$\text{COP} = \frac{\dot{Q}_e}{\dot{Q}_g + \dot{W}_p} \quad (\text{eq. 5})$$

$$\text{CR} = \frac{m_3}{m_9} \quad (\text{eq. 6})$$

An important parameter is the cut-off temperature of the cycle, which is the minimum generator temperature needed for the system to operate at given conditions. Two parametric studies were developed: the first one considering that the equilibrium temperature at the outlet of the absorber and condenser (T_1 and T_8), called intermediate temperature (T_{int}), is fixed at 40°C . The second case assumes two fixed generator outlet temperatures ($T_7 = T_g$): 75°C and 85°C .

2.4 Results and discussion

The comparison of COP vs T_{int} for the $\text{NH}_3\text{-H}_2\text{O}$, $\text{NH}_3\text{-LiNO}_3$, and $\text{H}_2\text{O-LiBr}$ working pairs can be observed in Figure 5. As the intermediate temperature increases, the COP decreases. In the case of the outlet generator temperature of 75°C , the machine is able to operate at maximum intermediate temperatures T_{int} of 40°C , 41°C , and 40.5°C for the $\text{NH}_3\text{-H}_2\text{O}$, $\text{NH}_3\text{-LiNO}_3$, and $\text{H}_2\text{O-LiBr}$ working fluids, respectively. As the intermediate temperature gets close to its higher limit, the COP decreases drastically. Hence, it is recommended to limit the operating intermediate temperatures to keep acceptable COP values (of around 0.6) at T_{int} of 37°C , 39°C , and 40°C or less for the $\text{NH}_3\text{-H}_2\text{O}$, $\text{NH}_3\text{-LiNO}_3$, and $\text{H}_2\text{O-LiBr}$ cycles, respectively.

An increase in the generator temperature leads to higher allowable intermediate temperatures. When the generator temperature is increased to 85°C , the machine is able to operate at maximum intermediate temperatures T_{int} of 44°C , 46°C , and 45°C for the $\text{NH}_3\text{-H}_2\text{O}$, $\text{NH}_3\text{-LiNO}_3$, and $\text{H}_2\text{O-LiBr}$ working fluids, respectively. Moreover, in order to maintain a COP of at least 0.6, a T_{int} of 39°C , 42°C , and 44°C or less is required for the $\text{NH}_3\text{-H}_2\text{O}$, $\text{NH}_3\text{-LiNO}_3$, and $\text{H}_2\text{O-LiBr}$ cycles, respectively. For both generator temperatures, the $\text{H}_2\text{O-LiBr}$ working fluid is the working pair that can operate at highest intermediate temperatures with acceptable COP values. Moreover, as observed in Figures 1 and 2, a generator operating temperature higher than 75°C would be recommended, as lower generator temperatures limit the intermediate temperature to conditions that might not be achievable in real applications. In the optimum operating temperature conditions of $T_{int} = 40^\circ\text{C}$ and $T_g = 85^\circ\text{C}$, the $\text{H}_2\text{O-LiBr}$ working fluid shows the highest COP.

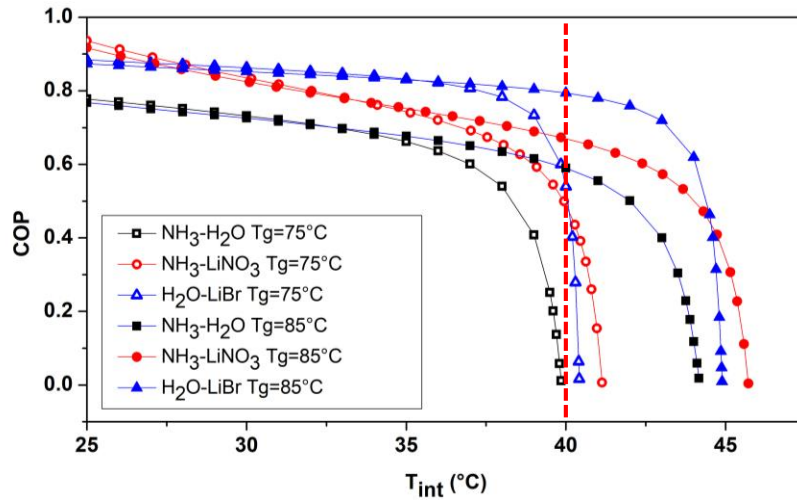


Fig. 5: Effect of T_{int} on COP at $T_e=10^\circ\text{C}$ and two different generator temperatures ($T_g=75^\circ\text{C}$ and $T_g=85^\circ\text{C}$).

Figure 6 shows the effect of the intermediate temperature on the circulation ratio (CR) at two different outlet generator temperatures (75°C and 85°C). As the generator temperature increases, the circulation ratio also increases, and a higher circulation ratio requires more pumping capacity. Therefore, it is not recommended to operate the system at high intermediate temperatures. In the range of low intermediate temperatures, $\text{NH}_3\text{-LiNO}_3$ possesses the highest circulation ratios, and $\text{NH}_3\text{-H}_2\text{O}$ the lowest.

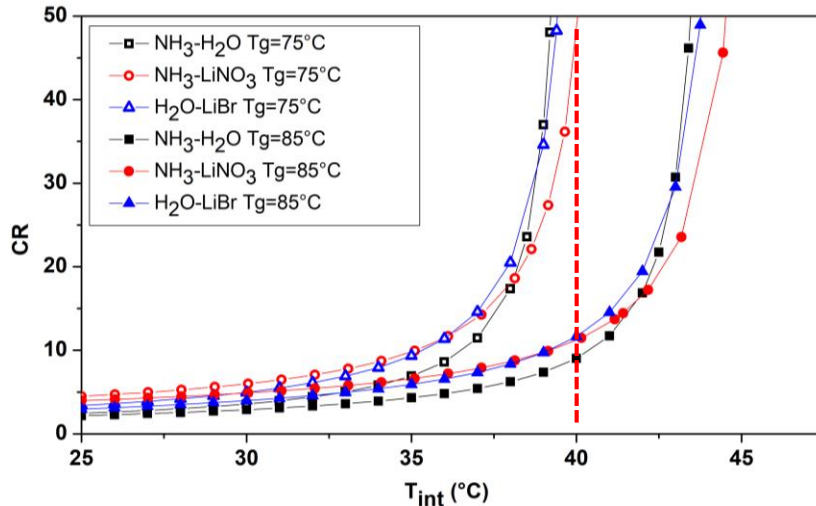


Fig. 6: Effect of T_{int} on Circulation Ratio at $T_e=10^\circ\text{C}$ and two different generator temperatures ($T_g=75^\circ\text{C}$ and $T_g=85^\circ\text{C}$).

Figure 7 shows the COP variations comparison against generator temperatures, considering an intermediate temperature of 40°C . The hot water storage unit is able to provide heat transfer fluid in the range of $70\text{-}100^\circ\text{C}$. The compared systems have different cut-off temperatures. In the case of the $\text{NH}_3\text{-H}_2\text{O}$ system, its cut-off temperature is of 75°C , while for $\text{H}_2\text{O-LiBr}$ it is of 74°C . Finally, $\text{NH}_3\text{-LiNO}_3$ possesses the lowest cut-off temperature of 72°C . However, it does not necessarily mean that it is the most convenient working fluid in the studied case, as the COP values of the three fluids increase dramatically just above the cut-off temperature. The value of the generator temperatures for which the system starts to operate at acceptable performances (COP values higher than 0.6) is about 75.5°C for the $\text{H}_2\text{O-LiBr}$ pair, 78°C for $\text{NH}_3\text{-H}_2\text{O}$, and 87°C for $\text{NH}_3\text{-H}_2\text{O}$. Moreover, the $\text{H}_2\text{O-LiBr}$ system reaches and maintains the highest COP values for the rest of the generating temperatures. This indicates that if a good control over the generating temperatures is maintained, the $\text{H}_2\text{O-LiBr}$ working fluid would be the most convenient for the studied case in terms of performance.

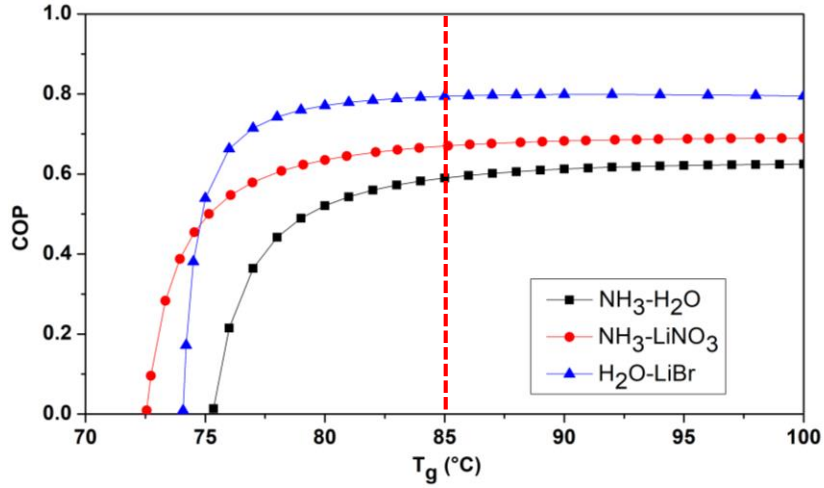


Fig. 7: Effect of T_g on COP at $T_e=10^\circ\text{C}$ and $T_{int}=40^\circ\text{C}$.

Figure 8 illustrates the impact of the generator temperature on the circulation ratio at $T_{int}=40^\circ\text{C}$ and $T_e=10^\circ\text{C}$. In the lower limit conditions of the generator temperatures, the circulation ratio increases drastically. Hence, higher generator temperatures are recommended. At high generator temperatures, the $\text{NH}_3\text{-H}_2\text{O}$ working pair has the lowest circulation ratios, and $\text{NH}_3\text{-LiNO}_3$ has the highest, but very close to the ones of $\text{H}_2\text{O-LiBr}$.

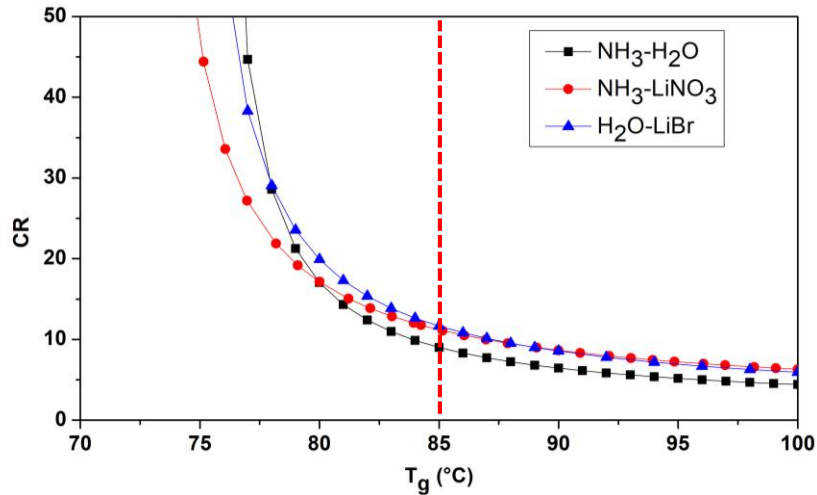


Fig. 8: Effect of T_g on COP at $T_e=10^\circ\text{C}$ and $T_{int}=40^\circ\text{C}$.

4. Integrated solar-geothermal absorption cooling system and economic feasibility study

4.1 Solar-geothermal absorption cooling system and dimensioning

Following the study of the cycle performances, the integration of the absorption cycle with the solar driving heat source and the geothermal heat sink source can be performed. The proposed configuration is the one illustrated in Figure 1. The system consists of a solar thermal evacuated tubes collector system, a hot water storage tank, the absorption chiller, the air handler, and a HGHE. In order to make an objective comparison of the proposed working fluids, an evaporator average power of 5 kW is fixed for the cooling system eight hours a day during the 6 hottest months in Monterrey (Apr-Sept), and an average solar irradiance of 1 kW/m² (which is acceptable according to Figure 2) was taken into account for these conditions. The total power to be put into the ground would be approximately $\dot{Q}_{int} = \dot{Q}_a + \dot{Q}_c$, while the power of the evacuated tube collectors is approximately \dot{Q}_g if we consider that there is a good match between the solar irradiation availability and the cooling need, therefore, the influence of the hot water storage tank over the system's thermal components would be negligible. These values depend on the performance of the different absorption working fluids. In order to evaluate the solar collector area (in m²) required for the system, the equations presented hereafter were used.

$$A = \frac{\dot{Q}_g}{G^* \cdot \eta_{col}} \quad (\text{eq. 7})$$

$$\eta_{col} = k(\theta) \cdot \eta_0 - a_1 \frac{T_m - T_a}{G^*} - a_2 \frac{(T_m - T_a)^2}{G^*} \quad (\text{eq. 8})$$

$$k(\theta) = 1 - 0.239 \left(\frac{1}{\cos\theta} - 1 \right) \quad (\text{eq. 9})$$

In the calculations, a tilt angle of the collector of 25° and south orientation were considered, which is the recommended tilt angle for Monterrey’s 25° 4’ north latitude. While the collector’s characteristics are the ones of the Thermomax – Mazdom vacuum tube solar collectors ($\eta_0 = 0.804$, $a_1 = 1.15 \frac{^\circ\text{C}\cdot\text{m}^2}{\text{kW}}$ and $a_2 = 0.0064 \frac{^\circ\text{C}\cdot\text{m}^2}{\text{kW}}$). In the case of the hot water storage tank, 60 liters were considered for every square meter of collector (Mateus and Oliveira, 2009). The work on the characterization and dimensioning of HGHE was presented in Moch’s thesis (2013) and was followed by other papers on the subject (Agbossou et al., 2018; Moch et al., 2015, 2014). This study concerns geothermal heat pumps, and more precisely the impact of the heat transfers on the underground temperature near the HGHE and the temperature provided to the heat pump. The transient calculations were performed considering coils of standard size (1 m diameter and 3 m height) inserted in a 4 m deep well and assuming a quasi-constant heat flux along the day, whereas in the present study, the absorption heat pump operates only during eight hours a day, which somewhat underestimates the underground temperature even if the energy exchanges per day are the same for the two studies. Considering a heat exchange during the 6 hottest months of the year (Apr-Sept) with no phase change and a dry underground (worst case scenario for the thermal transfers), Moch’s model leads to a capacity of 500 W for every helicoidal GHX and a separation of 4 meters between them to maintain a soil temperature perturbation under 9°C, that means a temperature of 33°C at the HGHE position (see Section 2). To calculate the surface area required for the HGHE, the number of coils has to be multiplied then twice by 4 m. The final values for the different systems requirements are shown in Table 1.

Tab. 1: Requirements and dimensioning for the studied conditions and the three studied working fluids.

	NH₃-H₂O	NH₃-LiNO₃	H₂O-LiBr
COP	0.59	0.67	0.794
\dot{Q}_{int} (kW)	13	12.68	11.39
Number of HGHE coils	26	26	23
Surface required for the GHX (m²)	416	416	368
\dot{Q}_g (kW)	8.5	7.46	6.35
Solar collector area (m²)	15	13	11
Size of the hot water storage tank (m³)	1	1	1

4.2 Economic assessment

In spite of their low operating costs, the historical problem with solar absorption air conditioning has been the elevated initial investment. Therefore, an analysis of the initial investment costs and economic benefits of the system becomes fundamental. Three fundamental economic parameters were selected to evaluate the economic performance of the selected system: The Net Present Value (NPV), the payback period (PB), and the Return On Investment (ROI). In order to be a profitable system, the NPV should be positive, the PB should be at least half of the product lifetime, and the ROI should be higher than one. The parameters used for the economic study are shown in Table 2.

Tab. 2: Economic data for the initial investment of the solar-geothermal absorption cooling system.

Concept	Data
Lifetime of absorption systems (years)	20 (Tsoutsos et al., 2003)
Inflation rate for the year 2017 (%)	6.77 (“Banco de México,” 2018)
Price of electricity (USD/kWh)	0.1484 (“CFE,” 2018)
Average energy inflation in Mexico from 2006 to 2017 (%)	2.62 (“CFE,” 2018)

The Mexican pesos – USD exchange rate considered was 1 MXN = 0.053 USD. The system’s cost of installation (not including the GHX) was considered to be 30% of the cost of the chiller and the hot storage tank was priced at 2600 USD/m³ (Viñas et al., 2016). The solar collectors were priced at 200 USD/m² and the absorption chiller at 572

USD/kW (Vargas Bautista et al., 2011). The electricity consumption by the pumps and auxiliary elements was neglected considering the orders of magnitude of the other economic parameters. Finally, regarding the geothermal installation, a cost of 1,500 USD for every 100 m² of 4 m depth GHE was calculated (Acuña et al., 2017). Taking the presented economic parameters and the chillers operating conditions presented in Section 4.1, the annual economic benefits were calculated by considering the energy savings and the operational costs. With the new energy reform in Mexico, new programs are being implemented to promote the use of renewable energies in the country. This is why for the economic evaluation; two scenarios were considered. In the first one, the user would cover the entire investment costs of the system, and in the second scenario, the government would subsidize 40% of it. The considered costs for the initial investment are presented in Table 3.

Tab. 3: Considered costs for the initial investment of the solar-geothermal absorption cooling system and economic analysis considering two scenarios.

		NH₃-H₂O	NH₃-LiNO₃	H₂O-LiBr
Initial investment	<i>Absorption chiller</i>	\$2,860.00	\$2,860.00	\$2,860.00
	<i>GHX construction and installation</i>	\$6,240.00	\$6,240.00	\$5,520.00
	<i>Solar evacuated tube collectors</i>	\$3,000.00	\$2,600.00	\$2,200.00
	<i>Hot storage tank</i>	\$2,600.00	\$2,600.00	\$2,600.00
	<i>System installation costs</i>	\$2,000.00	\$2,000.00	\$2,000.00
	<i>Required pumps</i>	\$604.00	\$604.00	\$604.00
	<i>Air handling unit</i>	\$1,500.00	\$1,500.00	\$1,500.00
	<i>Accessories</i>	\$1,200.00	\$1,200.00	\$1,200.00
	TOTALS	\$20,004.00	\$19,604.00	\$18,484.00
	TOTALS WITH SUBVENTION 40%	\$12,002.40	\$11,762.40	\$11,090.40
SCENARIO 1	<i>NPV</i>	-\$2,985.57	-\$2,585.57	-\$1,465.57
	<i>PB</i>	18.08	17.72	16.71
	<i>ROI</i>	1.10	1.13	1.19
SCENARIO 2	<i>NPV</i>	\$5,016.03	\$5,256.03	\$5,928.03
	<i>PB</i>	10.86	10.64	10.03
	<i>ROI</i>	1.84	1.88	1.99

From the results in Table 3, the scenario 1 would not be economically viable, as the NPV results negative and the payback period is almost the same as the system's lifetime. As observed by the ROI, at the end of the product lifetime, there is almost no economic gain. On the other hand, the second scenario seems economically viable, as the systems pay themselves after around 10 or 11 years of operation and their NPV is positive. In order to make use of the system in other than hot months in Mexico, its use for domestic hot water production should be considered. Finally, the application of a solar-geothermal system like the one presented here in Mexico could only be viable in the current market conditions if new green subsidies are offered to the families, otherwise, the implementation is possible, but seems like not economically viable.

5. Conclusion and perspectives

A small-capacity geothermally-cooled absorption system for hot climates has been proposed. The functioning of this system in the Monterrey city (Mexico) climate conditions has been analyzed. Three working fluids were studied as possible candidates, the two conventional NH₃-H₂O and H₂O-LiBr working fluids and a third innovative working fluid (NH₃-LiNO₃). In a first section, the climatic conditions of Monterrey were studied to see how they impact the operating temperatures of the system. In a second section, the thermodynamic cycle performances for the three proposed working fluids were compared. Finally, the dimensioning of the components of the solar-geothermal system and an economic viability study was performed, to see if the proposed system could be cost-effective. A characteristic of the present study is that for the heat sink, a recently studied helical geothermal heat exchanger was considered, and the effects of the heat transfers on the underground temperature profiles were taken into account in the dimensioning to maintain a soil temperature perturbation under 9°C.

In terms of thermodynamic performance, the H₂O-LiBr resulted to be the most performant working pair for the nominal conditions. However, from the economic point of view and under the hypothesis considered for the present study, the choice of the working fluid seems to have a relatively low impact on the initial investment cost of a small-capacity solar-geothermal absorption system. On the other hand, the proposed system would be technically feasible,

but seems like not economically viable in the Mexican conditions. The geothermal system strongly impacts the already high initial investment cost of the solar absorption system. One option to increase the system's economic viability would be to take into account the use of the solar thermal collectors and the hot water storage tank as domestic hot water because, in arid regions like northern Mexico, the need for heating is also important during winter. However, other aspects in terms of security and technical requirements must be compared for the different working fluids to observe if there is one with the most ideal conditions for the Mexican climate requirements. In the context of the recently implemented Mexican energy reform, there is a big expectation and new implementation of programs to transit to a more sustainable energy market. New green subsidies could be an important factor to boost this transition and engage Mexicans in the challenge. The present study aims to provide the orders of magnitude of the technical and economic perspectives of a solar-geothermal absorption cooling system implemented in the northern region of Mexico. A more complex analysis would have to be developed before the implementation of a real machine with real quotations and more detailed calculations of its operation.

Acknowledgements

The present work was supported by the Sectorial Fund "CONACYT – SENER – SUSTENTABILIDAD ENERGÉTICA".

6. References

- Acuña, A., Lara, F., Rosales, P., Suastegui, J., Velázquez, N., Ruelas, A., 2017. Impact of a vertical geothermal heat exchanger on the solar fraction of a solar cooling system. *Int. J. Refrig.* 76, 63–72. <https://doi.org/10.1016/j.ijrefrig.2017.02.007>
- Agbossou, A., Souyri, B., Stutz, B., 2018. Modelling of helical coil heat exchangers for heat pump applications: Analysis of operating modes and distance between heat exchangers. *Appl. Therm. Eng.* 129, 1068–1078. <https://doi.org/10.1016/j.applthermaleng.2017.10.089>
- Agrouaz, Y., Bouhal, T., Allouhi, A., Kousksou, T., Jamil, A., Zeraouli, Y., 2017. Case Studies in Thermal Engineering Energy and parametric analysis of solar absorption cooling systems in various Moroccan climates. *Case Stud. Therm. Eng.* 9, 28–39. <https://doi.org/10.1016/j.csite.2016.11.002>
- Aliane, A., Abboudi, S., Seladji, C., Guendouz, B., 2016. An illustrated review on solar absorption cooling experimental studies. *Renew. Sustain. Energy Rev.* 65, 443–458. <https://doi.org/10.1016/j.rser.2016.07.012>
- Allouhi, A., Fouih, Y. El, Kousksou, T., Jamil, A., Zeraouli, Y., Mourad, Y., 2015. Energy consumption and efficiency in buildings : current status and future trends. *J. Clean. Prod.* 109, 118–130. <https://doi.org/10.1016/j.jclepro.2015.05.139>
- Bailo, C.M., Garcés, S.A., Arizón, F.P., 2010. Analysis of a New Dissipation System for a Solar Cooling Installation. *J. Thermodyn.* 2010, 1–6. <https://doi.org/10.1155/2010/750675>
- Banco de México [WWW Document], 2018. . Inflación. URL <http://www.anterior.banxico.org.mx/portal-inflacion/inflacion.html>
- Best, R., Rivera, W., 2015. A review of thermal cooling systems. *Appl. Therm. Eng.* 75, 1162–1175. <https://doi.org/10.1016/j.applthermaleng.2014.08.018>
- Calm, J.M., 2008. The next generation of refrigerants - Historical review, considerations, and outlook. *Int. J. Refrig.* 31, 1123–1133. <https://doi.org/10.1016/j.ijrefrig.2008.01.013>
- Cera-Manjarres, A., Salavera, D., Coronas, A., 2018. Vapour pressure measurements of ammonia/ionic liquids mixtures as suitable alternative working fluids for absorption refrigeration technology. *Fluid Phase Equilib.* <https://doi.org/10.1016/j.fluid.2018.01.006>
- CFE [WWW Document], 2018. . Tarifas. URL https://app.cfe.mx/aplicaciones/ccfe/tarifas/tarifas/tarifas_casa.asp
- Chen, J.F., Dai, Y.J., Wang, R.Z., 2017. Experimental and analytical study on an air-cooled single effect LiBr-H₂O absorption chiller driven by evacuated glass tube solar collector for cooling application in residential buildings. *Sol. Energy* 151, 110–118. <https://doi.org/10.1016/j.solener.2017.05.029>
- Doughty, C., Nir, A., Tsang, C.-F., 1991. Seasonal Thermal Energy Storage in Unsaturated soil : Model Development and Field Validation Soils:
- Dube, E., Cha, A., Agboola, O.P., Or, J., Fakeeha, A.H., Al-fatesh, A.S., 2017. Energetic and exergetic analysis of solar-powered lithium bromide- water absorption cooling system. *J. Clean. Prod.* 151, 60–73. <https://doi.org/10.1016/j.jclepro.2017.03.060>

- Farshi, L.G., Infante Ferreira, C.A., Mahmoudi, S.M.S., Rosen, M.A., 2014. First and second law analysis of ammonia/salt absorption refrigeration systems. *Int. J. Refrig.* 40, 111–121. <https://doi.org/10.1016/j.ijrefrig.2013.11.006>
- Hassan, H.Z., Mohamad, A.A., 2012. A review on solar cold production through absorption technology. *Renew. Sustain. Energy Rev.* 16, 5331–5348. <https://doi.org/10.1016/j.rser.2012.04.049>
- Hernández-Magallanes, J.A., Rivera, W., Coronas, A., 2017. Comparison of single and double stage absorption and resorption heat transformers operating with the ammonia-lithium nitrate mixture. *Appl. Therm. Eng.* 125, 53–68. <https://doi.org/10.1016/j.applthermaleng.2017.06.130>
- Ibrahim, O.M., Klein, S.A., 1993. Thermodynamic Properties of Ammonia—Water Mixtures. *ASHRAE Trans.* 99, 1495–1502.
- IEA, 2016. World energy outlook.
- Mateus, T., Oliveira, A.C., 2009. Energy and economic analysis of an integrated solar absorption cooling and heating system in different building types and climates. *Appl. Energy* 86, 949–957. <https://doi.org/10.1016/j.apenergy.2008.09.005>
- Moch, X., 2013. Étude théorique et expérimentale d'échangeurs géothermiques hélicoïdaux: Production de chaud et de froid par pompe à chaleur, et dimensionnement d'installations. Université de Grenoble.
- Moch, X., Palomares, M., Claudon, F., Souyri, B., Stutz, B., 2015. Geothermal helical heat exchangers: Coupling with a reversible heat pump in Western Europe. *Appl. Therm. Eng.* 81, 368–375. <https://doi.org/10.1016/j.applthermaleng.2015.01.072>
- Moch, X., Palomares, M., Claudon, F., Souyri, B., Stutz, B., 2014. Geothermal helical heat exchangers: Comparison and use of two-dimensional axisymmetric models. *Appl. Therm. Eng.* 73, 689–696. <https://doi.org/10.1016/j.applthermaleng.2014.06.051>
- Monné, C., Alonso, S., Palacín, F., Serra, L., 2011. Monitoring and simulation of an existing solar powered absorption cooling system in Zaragoza (Spain). *Appl. Therm. Eng.* 31, 28–35. <https://doi.org/10.1016/j.applthermaleng.2010.08.002>
- Noorollahi, Y., Saeidi, R., Mohammadi, M., Amiri, A., Hosseinzadeh, M., 2018. The effects of ground heat exchanger parameters changes on geothermal heat pump performance – A review. *Appl. Therm. Eng.* 129, 1645–1658. <https://doi.org/10.1016/j.applthermaleng.2017.10.111>
- Pátek, J., Klomfar, J., 2006. A computationally effective formulation of the thermodynamic properties of LiBr-H₂O solutions from 273 to 500 K over full composition range. *Int. J. Refrig.* 29, 566–578. <https://doi.org/10.1016/j.ijrefrig.2005.10.007>
- SIMA, 2018. Reportes mensuales de calidad del aire.
- SMN, 2018. Información Climatológica por Estado.
- Tillner-Roth, R., Harms-Watzenberg, F., Baehr, H.D., 1993. Eine neue fundamentalgleichung für ammoniak. *Dkv-taungsbericht* 20, 167–181.
- Tsoutsos, T., Anagnostou, J., Pritchard, C., Karagiorgas, M., Agoris, D., 2003. Solar cooling technologies in Greece. An economic viability analysis. *Appl. Therm. Eng.* 23, 1427–1439. [https://doi.org/10.1016/S1359-4311\(03\)00089-9](https://doi.org/10.1016/S1359-4311(03)00089-9)
- Ullah, K.R., Saidur, R., Ping, H.W., Akikur, R.K., Shuvo, N.H., 2013. A review of solar thermal refrigeration and cooling methods. *Renew. Sustain. Energy Rev.* 24, 499–513. <https://doi.org/10.1016/j.rser.2013.03.024>
- Vargas Bautista, J.P., García Cuéllar, A.J., Rivera Solorio, C.I., 2011. Design and economic analysis of a solar air-conditioning system: case of study in Monterrey, Mexico, in: *EUROSUN 2011*.
- Viñas, E., Best, R., Lugo, S., 2016. Simulation of solar air conditioning systems in coastal zones of Mexico. *Appl. Therm. Eng.* 97, 28–38. <https://doi.org/10.1016/j.applthermaleng.2015.09.104>
- Wu, W., Wang, B., Shi, W., Li, X., 2014a. An overview of ammonia-based absorption chillers and heat pumps. *Renew. Sustain. Energy Rev.* 31, 681–707. <https://doi.org/10.1016/j.rser.2013.12.021>
- Wu, W., You, T., Wang, B., Shi, W., Li, X., 2014b. Evaluation of ground source absorption heat pumps combined with borehole free cooling. *Energy Convers. Manag.* 79, 334–343. <https://doi.org/10.1016/j.enconman.2013.11.045>
- Zhu, L., Gu, J., 2010. Second law-based thermodynamic analysis of ammonia/sodium thiocyanate absorption system. *Renew. Energy* 35, 1940–1946. <https://doi.org/10.1016/j.renene.2010.01.022>